Experimental Investigation And Validation of Neutral Beam Current Drive for ITER through ITPA Joint Experiments

T. Suzuki 1), R. J. Akers 2), D. A. Gates 3), S. Günter 4), W. W. Heidbrink 5), J. Hobirk 4), T. C. Luce 6), M. Murakami 7), J. M. Park 7), M. Turnyanskiy 2), and the ITPA "Integrated Operation Scenarios" group members and experts

1) Japan Atomic Energy Agency, 801-1, Mukoyama, Naka, Ibaraki-ken 311-0193, Japan
2) CCFE/EURATOM Fusion Association, Culham Science Centre, Abingdon, UK
3) Princeton Plasma Physics Laboratory, Princeton, USA
4) Max-Planck-Institut für Plasmaphysik, EURATOM Association, Garching, Germany
5) University of California, Irvine, USA
6) General Atomics, San Diego, USA
7) Oak Ridge National Laboratory, Oak Ridge, USA

e-mail contact of main author: suzuki.takahiro@jaea.go.jp

Abstract. Joint experiments investigating the off-axis neutral beam current drive (NBCD) capability to be utilized for advanced operation scenario development in ITER were conducted in 4 tokamaks (ASDEX Upgrade (AUG), DIII-D, JT-60U, and MAST) through the international tokamak physics activity (ITPA). The following results were obtained in the joint experiments, where the toroidal field, B_t, covered 0.4-3.7 T, the plasma current, I_p, 0.5-1.2 MA, and the beam energy, E_b, 48-350 keV. A current profile broadened by off-axis NBCD was observed in MAST. In DIII-D and JT-60U, NB driven current profile has been evaluated using motional Stark effect diagnostics and good agreement between the measured and calculated NB driven current profile was observed. In AUG (at low δ~0.2) and DIII-D, introduction of a fast-ion diffusion coefficient of D_b~0.3-0.5 m^2/s in the calculation gave better agreement at high heating power (5 MW and 7.2 MW, respectively), suggesting anomalous transport of fast-ions by turbulence. It was found through these ITPA joint experiments that NBCD related physics quantities reasonably agree with calculations (with D_b=0-0.5 m^2/s) in all devices when there is no MHD activity except ELMs.

1. Introduction and Background of NBCD Validation Efforts

NBCD is the main current drive source in ITER. In order to reach a steady-state operation scenario free from low m & n MHD activity (e.g. neo-classical tearing mode (NTM) etc.) that is resonant on low q rational surfaces, it is expected that $q_{min} > $ ~1.5. Off-axis current drive is essential to sustain such weak or reversed magnetic shear. The negative ion-source based NB (N-NB) injector has been designed with off-axis steering capability in ITER, and the characteristics of off-axis NBCD are of great concern to achieve a Q=5 steady-state operation scenario in ITER. Concerning on-axis NBCD, the measured NBCD profile at E_b up to 370 keV using an ITER-relevant N-NB system in JT-60U showed good agreement with calculations [1,2]. However, there had been no result on off-axis NBCD profile, which is more important for current profile control in the steady-state operation scenario. AUG first reported off-axis NBCD from the viewpoint of current profile tailoring, where the measured off-axis NBCD current did not agree with calculations and was smaller than the calculation [3] in the case of strong heating into a low δ plasma. Later, the difference was attributed to possible diffusive redistribution of fast-ions by turbulence [4]. JT-60U also investigated the off-axis NBCD and found good agreement between measurement and calculation of the off-axis NBCD current, but found a difference in the NBCD location [5]. Thus, joint experiments were conducted through the ITPA to validate off-axis NBCD capability. This paper reports on the results of the joint experiments conducted in 4 tokamaks, AUG, DIII-D, JT-60U, and MAST. Since it is known that MHD activity bring about redistribution of fast-ions and modify the NBCD capability, these joint experiments were

TABLE I: OPERATION PARAMETERS AND SUMMARY OF THE OFF-AXIS NBCD JOINT EXPERIMENT.

Device	AUG	DIII-D	JT-60U	MAST
I_p [MA]	0.6-0.8	0.9	1.2	0.5-0.8
B_t [T]	2-2.5	2.1	~3.7	0.4-0.5
R_p [m]	~1.65	~1.7	~3.3-3.4	~0.85
a [m]	~0.5	0.55	~0.8-0.9	~0.65
triangularity δ (ave.)	0.2-0.4	0.57	0.25-0.45	~0.35
E_b [keV]	93	81	85, 350(N-NB)	48, 65
r/a of off-axis NBCD peak in calculation	~0.55	~0.5	~0.3(N-NB)-0.6	~0.5
the way of realizing off-axis NBCD	up/downward-steered off-axis beams	up/down-shift of the plasma	downward-steered off-axis beams	up/down-shift of plasma
codes for comparison	TRANSP	NUBEAM,TRANSP	ACCOME	TRANSP
summary of results	agreement (but D_b=0.5 m^2/s at low δ=0.2 and 5MW heating power)	agreement in j_{BD} (but D_b=0.3 m^2/s at 7.2 MW heating power)	agreement in NBCD location over wide range of parameter scan	broader j profile by off-axis NBCD

conducted in plasmas without MHD activity (e.g. sawteeth, fishbones, NTMs, Alfvén eigenmodes) except ELMs.

2. Experimental Conditions of Off-axis NBCD

Operation parameters of the devices for off-axis NBCD (as well as on-axis NBCD for comparison) are shown in Table 1. Positive-ion based NB's (E_b<100 keV) are used in all devices, as well as N-NB (E_b~350 keV) in JT-60U. Plasma size, shape and magnetic field vary, and the way off-axis NB injection is realized varies from device to device; use of off-axis steered NBs in AUG (up/downward) and JT-60U (downward), and vertical shift of the plasma in DIII-D (up/downward) and MAST (downward). Figure 1 shows the beam lines for off-axis NBCD in all devices and their relative position to the plasma. Locations of off-axis NBCD using positive-ion based NB (P-NB) are intended to be about a half minor radius (r/a~0.5) in all devices. In addition, off-axis NBCD at r/a~0.3 was performed in JT-60U N-NB case, which is closer to the off-axis steering NBCD in ITER. Since half of the N-NB (lower ion source injected upward) is almost on-axis (Fig. 1 (c)), only the other half (upper ion source injected downward) was used for this study. MHD activity that redistributes fast-ions is avoided during NBCD analysis by adjusting operation scenarios, for example, high q_{95} operation (up to ~6) and/or pre-heating during current ramp-up to delay current
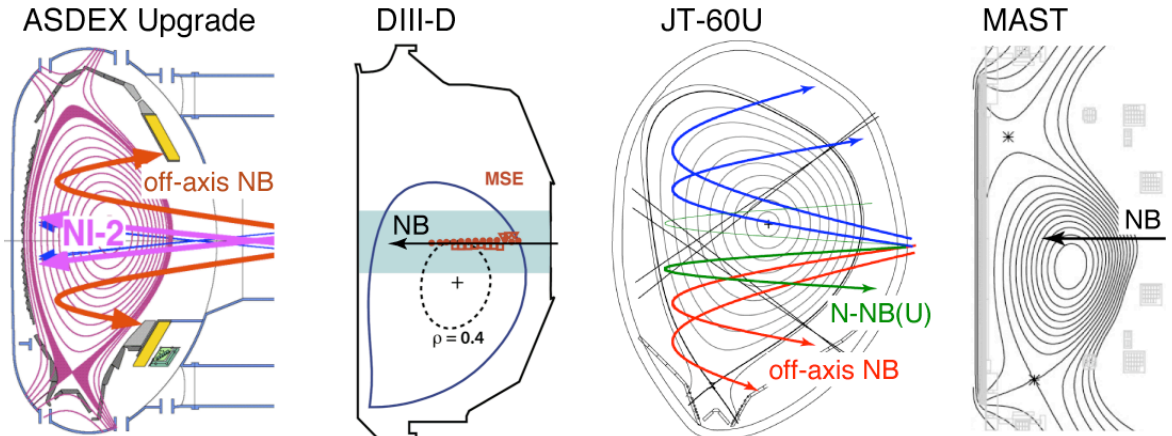

FIG. 1. Beam lines for off-axis NBCD in 4 devices and their position with respect to plasma. AUG and JT-60U have exclusive off-axis beam lines, while DIII-D and MAST realized off-axis NBCD by vertical shift of the plasma.
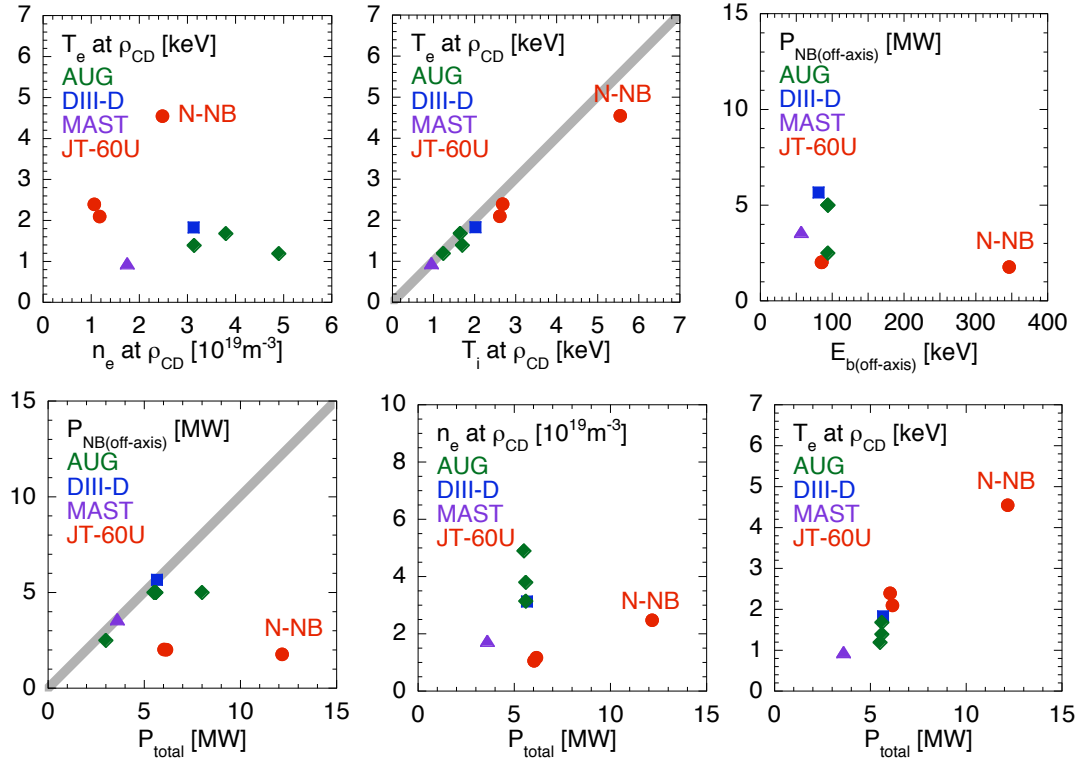
FIG. 2. (a), (b) Operation regime of off-axis NBCD experiments over electron density and ion/electron temperatures at the NBCD location ρ_{CD} defined as the peak location of the beam driven current density in each calculation. In this paper, symbol shapes and colors indicate devices (AUG: green diamonds, DIII-D: blue squares, MAST: violet triangles, JT-60U: red circles). (c) Relation between off-axis NBCD power and the off-axis beam energy E_b. (d) Relation between off-axis NBCD power and total heating power P_{total}. Gray line in (d) indicates that all heating power comes from the off-axis NBCD power. (e) Electron density and (f) electron temperature as a function of P_{total}.

penetration. In all devices, the NB driven current or change in the current profile by NB driven current is measured directly using motional Stark effect (MSE) diagnostics. The measured results are compared with theoretical calculations that are different between devices as shown in Table I. There was a detailed benchmarking study between some NBCD codes using parameters of the reference ITER steady state scenario [6], where the calculated beam driven current profiles by the ACCOME and NUBEAM codes give reasonable agreement (Fig. 2 in ref. 6).

3. Experimental Results

In the beginning of this section, plasma parameters (electron density n_e, electron temperature T_e and ion temperature T_i) during off-axis NBCD are summarized in Fig. 2 (a) and (b). The parameters are measured at the NBCD location ρ_{CD} defined as the peak location of the beam driven current density in each calculation. Figures 2 (c) and (d) show the relation of off-axis NBCD beam energy E_b, off-axis NBCD power $P_{NB(off-axis)}$ and total heating power P_{total}. Thanks to the joint experiments, wide dynamic ranges of the local plasma parameters as well as global parameters (Table I) have been achieved. Figure 2 (e) and (f) shows n_e and T_e as a function of P_{total}. Roughly speaking, higher T_e was obtained at larger P_{total}. In the following, off-axis NBCD measurements in such plasmas are described in detail.

In MAST, the radial profile of the plasma current density was measured in a nearly

Ohmic discharge as well as off-axis NBCD discharges [7]. A significant change in the MSE polarization angle (proportional to the magnetic field pitch angle viewed from the MSE optics) between Ohmic and off-axis NBCD discharges was observed in Fig. 3 (a). The resulting plasma current density profile broadened in the off-axis NBCD phase relative to the Ohmic phase at similar $n_e \sim 2 \times 10^{19}$ m^{-3} as shown in Fig. 3 (b). In the off-axis NBCD discharge at higher $n_e \sim 4 \times 10^{19}$ m^{-3}, the current density profile broadened less than at lower n_e, showing a reduction in the off-axis beam driven current with increasing n_e, qualitatively consistent with theory.

A more direct comparison of the beam driven current profile, j_{BD}, was done in DIII-D [8] and JT-60U, using loop-voltage-profile analysis [9]. Figure 4 shows the comparison between measurement and calculation in JT-60U (2.0 MW off-axis NBCD) and DIII-D (5.6 MW off-axis NBCD), as well as ITER-like slightly off-axis NBCD ($\rho_{CD} \sim 0.3$) using N-NB (1.8 MW, ~350 keV) in JT-60U. The codes used for the calculations in JT-60U and DIII-D are ACCOME and NUBEAM, respectively.
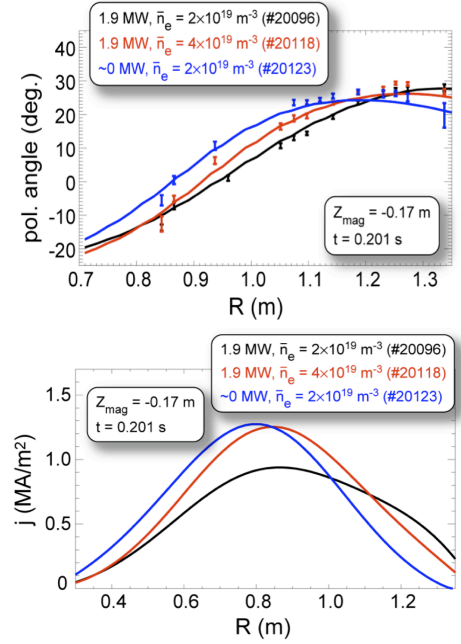
FIG. 3. (a) MSE polarization angle and (b) current density j profile measured by MSE in MAST for nearly Ohmic (blue) and NBCD phases (red: higher n_e, black: lower n_e), showing the difference in j broadened by off-axis NBCD.
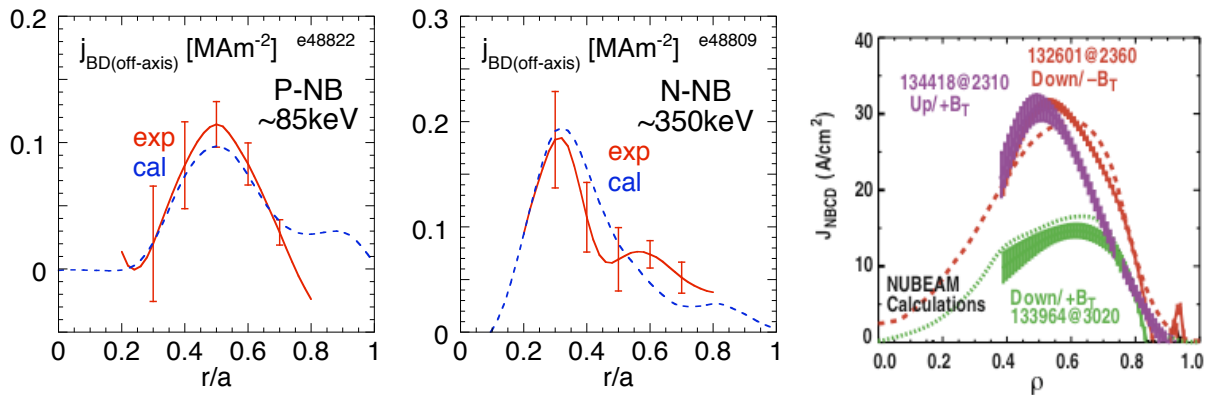
Characteristic profile shapes and magnitudes of the beam driven current density in calculations are well validated by the measurements in Fig. 4. Figure 5 shows the comparisons of area-integrated beam driven current I_{BD} and NBCD location ρ_{CD} between measurement and calculation in DIII-D and JT-60U. AUG data plotted in Fig. 5 (a) are I_{BD} reproducing the measured surface loop-voltage in ASTRA code under Zeff that reproduces the surface loop-voltage in on-axis NBCD phase just before the off-axis NBCD phase. This is because MSE data are not available in AUG during off-axis NBCD phase, as described later. Agreement of I_{BD} between measurements and calculations are obtained within their error bars for each machine. However, in general trend in Fig. 5 (a), measured I_{BD} are lower than calculations in all devices.

FIG. 4. Comparison of the beam driven current density profile between measurement and calculation. (a) JT-60U P-NB ~85 keV, (b) JT-60U N-NB ~350 keV, (c) DIII-D ~81 keV. Good agreement is observed both in JT-60U and DIII-D. In DIII-D, NB injection angles to the magnetic field are scanned by changing the direction of the vertical shift and the direction of the toroidal magnetic field (3 cases are shown).
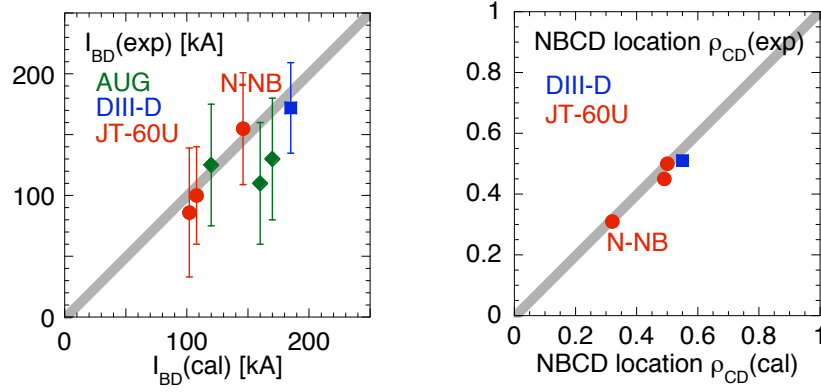
FIG. 5. (a) Comparison of measured beam driven current I_{BD} and calculated one (no radial diffusion of fast-ions is taken into account) in AUG, DIII-D and JT-60U. I_{BD} are integrated in a rage r/a=0.2-0.8 in Fig. 4 for JT-60U. (b) Comparison of NBCD location ρ_{CD} between measurement and calculation, defined as the peak location of the beam driven current density in calculation. Definition of the symbols is the same as Fig. 2.

NBCD current is theoretically predicted to depend on the NB injection angle to the magnetic field line [10,11]. In order to study the effect of NB injection angle, the direction of the toroidal magnetic field B_t, and the vertical shift of the plasma were scanned in DIII-D as shown in Fig. 4 (b). The measured beam driven current is almost the same between the up-shifted plasma with positive B_t and the down-shifted plasma with negative B_t, since the NB injection angles to the magnetic field line are the same. On the contrary, a significant decrease in the beam driven current was observed in the case of off-axis NBCD in the down-shifted plasma with positive B_t. These results validate the theoretical prediction.

In DIII-D, a discrepancy between the measured and calculated NB driven current (and profiles) was observed for higher heating power at 7.2 MW even without MHD activity when fast-ion diffusion coefficient $D_b=0$ is assumed (c.f. 5.6MW for Fig. 4 (c)). Figure 6 (a) shows a comparison of the measured and calculated beam driven current as a function of current drive power. As shown in the figure, disagreement appears at the highest power. The measured beam driven current profile at the highest power is shown in Fig. 6 (b), as well as calculations assuming various fast-ion diffusion coefficients. In this case, introducing a spatially uniform $D_b=0.3$ m^2/s gave better agreement than $D_b=0$, where not only redistribution but also loss of fast-ions are observed in the calculations with larger D_b [8]. This increased disagreement of the measured off-axis NBCD current and the corresponding calculation at higher heating power were also confirmed by other measurements of physics quantities characteristic of the fast-ion distribution function, which are the neutron emission and fast-ion
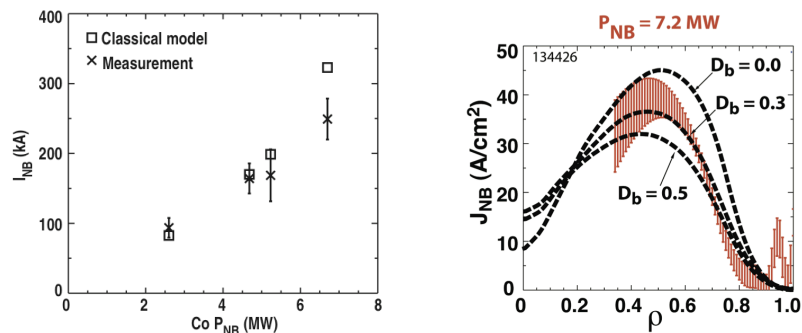

FIG. 6. (a) Measured and calculated beam driven current as a function of time (no radial diffusion of fast-ions is taken into account in the calculations) in DIII-D. (b) Comparison of the measured beam driven current density profile at 7.2MW NBCD and the corresponding calculations assuming various fast-ion diffusion coefficients D_b. Best agreement to the measurement is seen in $D_b=0.3$ m^2/s case.
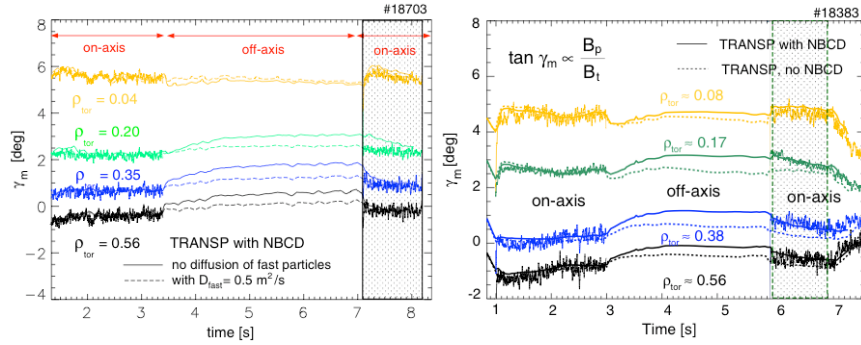
FIG. 7. Waveforms of MSE polarization angles in two AUG discharges at the same off-axis NBCD and heating powers (5MW and 5.6MW, respectively), but different triangularities (a) 0.2 and (b) 0.4. Since MSE diagnostic data are not available during off-axis NBCD in AUG, TRANSP simulation data adjusted before the start of off-axis NBCD are compared with MSE data after the end of off-axis NBCD. In the lower triangularity discharge, MSE measurements are not properly simulated for the $D_b=0$ assumed (solid curves). Better agreement between measurement and simulation was obtained for $D_b=0.5\ m^2/s$ (dotted curves). (b) In another higher triangularity discharge, MSE measurement are well simulated assuming $D_b=0$ (solid curves). Dotted curves correspond to no NBCD effect being taken into account in the simulation.

D_α (FIDA) measurements [12,13].

A similar result of the dependence of off-axis NBCD on heating power had already been observed at low-triangularity, δ~0.2, in AUG [4]. Figure 7 (a) shows the comparison of the temporal evolution of the MSE polarization angle (again, proportional to the magnetic field pitch angle viewed from the MSE optics) at various minor radii between the measurement and the TRANSP simulation. MSE data are not available during off-axis NBCD in AUG, because NTM appears when heating power increases with additional diagnostic NB for MSE. Thus, the measured MSE polarization angles are compared with the simulated ones in the decay phase after the end of off-axis NBCD in AUG. In a low-triangularity (δ=0.2) AUG discharge with 5.6 MW of heating power including 5 MW off-axis NBCD, good agreement between measurement and simulation was obtained assuming $D_b=0.5\ m^2/s$ than $D_b=0$ [4]. For lower off-axis NBCD and heating powers (2.5 MW and 3 MW, respectively), the off-axis NBCD effect was as expected in ASTRA simulations [14]. On the contrary to the low δ discharge, good agreement between MSE measurements and TRANSP simulations were observed in a higher δ=0.4 discharge (Fig. 7 (b)) at the same off-axis NBCD and heating powers as those in Fig. 7 (a). Diffusive redistribution of the fast-ions by turbulence was proposed as the cause in order to explain the observations in AUG [4].

4. Discussion

In the joint experiments described above, inability deterioration of off-axis NBCD has not been observed when there is no MHD activity except ELMs. In many cases, off-axis NBCD in a range r/a~0.3-0.5 agrees with theoretical calculations without introducing anomalous diffusion of fast-ions. In some devices and conditions (in AUG with low δ and in DIII-D), reasonably small D_b~0.3-0.5 m^2/s are required to obtain agreement between measurement and calculation at higher heating power (or off-axis NBCD power). After the work in AUG [4], there have been several theoretical works recently in the field of gyrokinetic simulation, simulating fast-ion transport induced by microturbulences [15-18]. The scalings of fast-ion diffusion coefficients based on the simulations are qualitatively similar to each other. The electrostatic diffusion of fast-ions in the background plasma with microturbulence approaches the diffusion of thermal-ions when the ratio of beam energy to the electron temperature of the background plasma (E_b/T_e) becomes smaller [15-18]. Since the
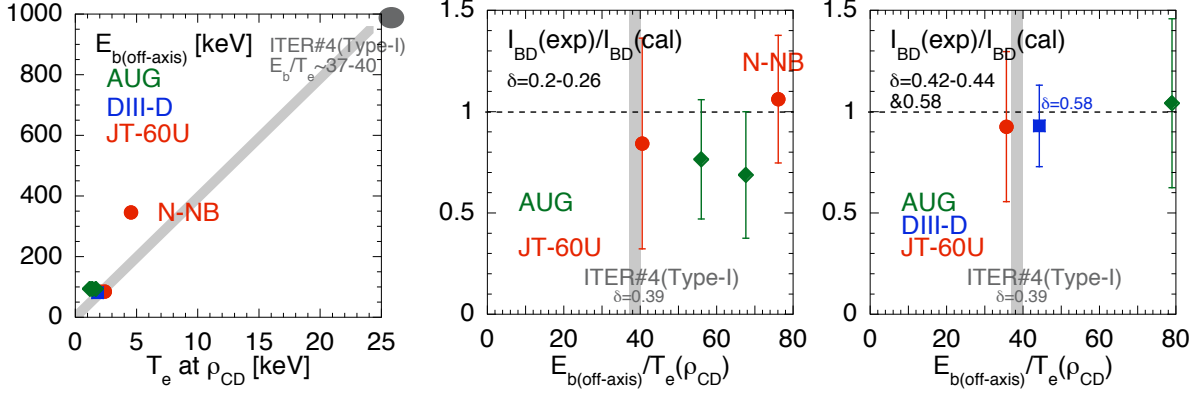
FIG. 8. (a) Conditions of off-axis NBCD experiments on beam energy E_b and T_e. (b) and (c): Measured off-axis beam driven current normalized by the theoretical calculation (no radial diffusion of fast-ions is taken into account) as a function of a parameter E_b/T_e. Low-triangularity case (b), and high-triangularity case (c). The gray shaded line shows the parameter range in E_b/T_e in ITER scenario #4 (Type-I) [19,20]. N-NB in JT-60U is for ρ_{CD}~0.3 and the others are for ρ_{CD}~0.5. Definition of the symbols is the same as Fig. 2.

thermal-ion diffusivity is, in general, larger off-axis than on-axis, the effect of microturbulence on fast-ion diffusion is significant for off-axis NBCD. In case of electromagnetic diffusion, the diffusion coefficient is independent of the beam energy and increases with plasma beta [18]. In this section, we discuss off-axis NBCD in ITER along such theoretical works, using the results in the ITPA joint experiments.

Figure 8 (a) shows the relation between the off-axis beam energy E_b (at injection) and T_e at the NBCD location ρ_{CD} in the joint experiments as well as one of the candidates for the ITER steady-state operation scenario (#4 Type-I) [19,20] for ρ_{CD}~0.2-0.3. The parameter E_b/T_e is estimated to be 37-40 for ITER conditions, and the results of joint experiments distribute around this value. In the joint experiments, lower E_b/T_e~40 near the ITER conditions are mostly obtained at higher T_e discharges with higher heating power in Fig. 2 (f). Figure 8 (b) and (c) plot the measured NBCD current normalized by the corresponding calculations for $D_b=0$ as a function of E_b/T_e in low and high-triangularity discharges, respectively. Separation of discharges depending on the triangularity is based on the AUG results in Fig. 7. It is considered that the ratio $I_{BD}(exp)/I_{BD}(cal)$ represents proximity to the $D_b=0$ condition. In either Fig. 8 (b) or (c) for ρ_{CD}~0.5, no clear dependence of the proximity on E_b/T_e as expected from the electrostatic diffusion of fast-ions is observed in the range of E_b/T_e shown here. It seems the proximity is worse in low-triangularity case (Fig. 8 (b)) than high-triangularity case (Fig. 8 (c)). According to reference [18], the δ of the ITER scenario is 0.39. Joint experiments for off-axis NBCD at r/a~0.5 with high-triangularity (Fig. 8 (c)) show agreement of I_{BD} between measurement and calculation with $D_b=0$ around E_b/T_e~37-40 (the upper bound by DIII-D and the lower bound by JT-60U). The off-axis NBCD profile for JT-60U is shown in Fig. 4 (a) where good agreement between the measurement and the calculation was obtained. In addition, off-axis steering of ITER N-NB is intended for ρ_{CD}~0.2-0.3, so the electrostatic effect of microturbulence is relatively smaller there than for ρ_{CD}~0.5 in the joint experiments due to the smaller thermal-ion diffusion at r/a~0.2-0.3. However, we must note that E_b/T_e in two AUG discharges shown in Fig. 7 are similar in a range 68-79, where the lower δ discharge (Fig. 7 (a)) requires $D_b=0.5$ m^2/s but the higher δ discharge (Fig. 7 (b)) requires no anomalous fast-ion diffusion. The value E_b/T_e~68 is much larger than that where DIII-D requires D_b~0.3m^2/s. Thus, we must keep in mind that there could be more hidden parameters, such as geometric ones like δ. In addition, in the AUG

discharges with similar E_b/T_e, higher toroidal beta discharge (1%, Fig. 7 (b)) requires $D_b=0$, while lower one (0.6%, Fig. 7 (a)) requires $D_b=0.5$ m^2/s. Thus, it seems it is difficult to understand from the viewpoint of electromagnetic diffusion of fast-ions alone. Further theoretical understanding of fast-ion transport and/or simulation work on realistic ITER geometry and parameter is necessary.

5. Summary

The following results were obtained in the ITPA joint experiments, where the toroidal field, B_t, covered 0.3-3.7 T, the plasma current, I_p, 0.6-1.2 MA, and the beam energy, E_b, 67-350 keV. The current profile was broadened by off-axis NBCD in MAST. In DIII-D and JT-60U, the NB driven current profile has been evaluated using motional Stark effect diagnostics and good agreement between the measured and calculated NB driven current profile was observed. In AUG (at low $\delta\sim 0.2$) and DIII-D, introduction of a fast-ion diffusion coefficient of $D_b\sim 0.3\text{-}0.5$ m^2/s in the calculation gave better agreement at high heating power (5 MW and 7.2 MW, respectively), suggesting anomalous transport of fast-ions by turbulence. It was found through these ITPA joint experiments that NBCD related physics quantities reasonably agree with calculations (with $D_b=0\text{-}0.5$ m^2/s) in all devices when there is no MHD activity except ELMs. Off-axis NBCD in ITER based on the ITPA joint experiments and a theoretically predicted scaling of fast-ion diffusion that depends on E_b/T_e or plasma beta has been discussed. However, in AUG, the fast-ion diffusion coefficient required to obtain a match between the measurements and calculations differs depending on δ even at similar E_b/T_e. Thus, we must keep in mind that there could be more hidden parameters, like δ. Further theoretical understanding of fast-ion transport and/or simulation work on realistic ITER geometry is necessary. The database obtained in the ITPA joint experiments here will provide such future work with a good touchstone of benchmarking with experimental measurements.

References
[1]   OIKAWA, T., et al., Nucl. Fusion **40** (2000) 435.
[2]   OIKAWA, T., et al., Nucl. Fusion **41** (2001) 1575.
[3]   HOBIRK, J., et al., 30th EPS Conference (2003) O-4.1B.
[4]   GÜNTER, S., et al., Nucl. Fusion **47** (2007) 920.
[5]   SUZUKI, T., et al., Nucl. Fusion **48** (2008) 045002.
[6]   OIKAWA, T., et al., *Proc. 22nd Int. Conf. on Fusion Energy 2008 (Geneva, 2008)* IT/P6-5.
[7]   TURNYANSKIY, M., et al., Nucl. Fusion **49** (2009) 065002.
[8]   PARK, J. M., et al., Phys. Plasmas **16** (2009) 092508.
[9]   FOREST, C. B., et al., Phys. Rev. Lett. **73** (1994) 2444.
[10] MURAKAMI, M., et al., Fusion Sci. Tech. **54** (2008) 994.
[11] MURAKAMI, M., et al., Nucl. Fusion **49** (2009) 065031.
[12] HEIDBRINK, W. W. et al., Phys. Rev. Lett. **103** (2009) 175001.
[13] HEIDBRINK, W. W. et al., Plasma Phys. Control. Fusion **51** (2009) 125001.
[14] GÜNTER, S., et al., 31st EPS Conference (2004) O-1.02.
[15] ZHANG, W., et al., Phys. Rev. Lett. **101** (2008) 095001.
[16] ZHANG, W., et al., Phys. Plasmas **17** (2010) 055902.
[17] HAUFF, T., et al., Phys. Plasmas **15** (2008) 112307.
[18] HAUFF, T., et al., Phys. Rev. Lett. **102** (2009) 075004.
[19] GORMEZANO, C. et al., Nucl. Fusion **47** (2007) S285.
[20] POLEVOI, A. R., et al., *Proc. 19th Int. Conf. on Fusion Energy 2002 (Lyon, 2002)* CT/P-08.